Distinct characteristics of dasatinib-induced pyroptosis in gasdermin E-expressing human lung cancer A549 cells and neuroblastoma SH-SY5Y cells

JUAN ZHANG, YANG CHEN and QIYANG HE

Institute of Medicinal Biotechnology, Peking Union Medical College and Chinese Academy of Medical Sciences, Beijing 100050, P.R. China

Received August 16, 2019; Accepted February 21, 2020

DOI: 10.3892/ol.2020.11556

Abstract. Dasatinib, a multikinase inhibitor, is used in the treatment of chronic myeloid leukemia and was developed to overcome imatinib resistance. Its mechanism of action involves the induction of apoptosis, autophagy and necroptosis. However, it remains unclear whether dasatinib can induce pyroptosis. In the present study, gasdermin E (GSDME)-expressing SH-SY5Y and A549 cells were chosen for investigation. Typical pyroptotic features, such as cleavage of GSDME protein, leakage of lactate dehydrogenase and large bubbled morphology, were observed in both cell lines after exposure to dasatinib. The generation of GSDME fragments was inhibited by specific caspase-3 inhibitor zDEVD in SH-SY5Y cells and pan-caspase inhibitor zVAD in A549 cells. Moreover, distinct characteristics of pyroptosis were observed in A549 cells, which occurred only with a high percentage of Annexin V/propidium iodide double-stained cells and low level of GSDME protein cleavage. The sensitivity of A549 cells to dasatinib is significantly reduced by increasing cell numbers. The elevation of GSDMD and GSDME protein levels was induced by low concentrations of dasatinib, which was not influenced by the reduction of p53 protein with RNA interference. In conclusion, to the best of our knowledge, this is the first study to report that dasatinib can induce pyroptosis in tumor cells and increase the protein levels of GSDMD and GSDME in a p53-independent manner.

Correspondence to: Professor Qiyang He, Institute of Medicinal Biotechnology, Peking Union Medical College and Chinese Academy of Medical Sciences, 1 Tiantan Xili, Beijing 100050, P.R. China
E-mail: qiyang_he@vip.163.com

Abbreviations: DOX, doxorubicin; GSDMD, gasdermin D; GSDME, gasdermin E; LDH, lactate dehydrogenase; PARP-1, poly (ADP-ribose) polymerase 1; PI, propidium iodide

Key words: pyroptosis, dasatinib, tumor cells, gasdermin D, gasdermin E, p53

Introduction

Dasatinib is a multikinase inhibitor, which has potent effects against chronic leukemia and used in cases of imatinib resistance as a second-generation targeted drug approved by the Food and Drug Administration (1,2). It has also been shown to act as potentiator of immunotherapy when used with an anti-PD-1 inhibitor and as a pharmacologic on/off switch for immune CAR-T cell activity (3,4). Moreover, dasatinib has been shown to promote the clearance of senescent cells, indicating its potential application in improving the overall health of older adults (5,6). Several molecular targets for dasatinib have been identified, including BCR-ABL fusion protein, Src and the collagen receptor discoidin domain receptor 2 (2,7,8). Accumulating data has demonstrated the mechanisms by which dasatinib actions are associated with the induction of apoptosis (9), autophagy (10) and necroptosis (11), depending on the cell type being targeted. However, it remains unclear whether dasatinib can evoke pyroptosis in tumor cells.

Pyroptosis, a mode of necrotic cell death, is characterized by cell swelling and the release of pro-inflammatory molecules due to pore formation in the cell membrane (12). One of the main family of proteins involved in pyroptosis are gasdermin proteins, cleavage fragments of these proteins insert into the cell membrane. Gasdermin D (GSDMD) mediates protection against bacterial infections, whereas gasdermin E (GSDME) is involved in chemotherapy-induced pyroptosis in tumor cells (13,14), which requires the activation of caspase-3. The expression of the GSDME gene is promoted by anti-oncogene p53 (15). Research has shown that targeted drugs can induce pyroptosis in cancer cells, such as trametinib in lung carcinoma cells, and cytotoxic antitumor agent 5-fluorouracil in gastric cancer cells (16,17).

In order to determine whether dasatinib can induce pyroptosis in tumor cells, two GSDME-expressing cell lines were chosen for the present study. These cell lines have previously been used to study chemotherapy-induced pyroptosis (13). To the best of our knowledge the present study demonstrates for the first time that dasatinib induces typical pyroptosis in human SH-SY5Y and A549 tumor cells.

Materials and methods

Drugs and chemicals. Dasatinib was purchased from Selleck Chemicals. A 40 mM solution was prepared in dimethyl sulfoxide and stored at -20˚C until use. Doxorubicin (DOX), specific caspase-3 inhibitor Z-DEVD-FMK (zDEVD) and pan-caspase inhibitor Z-VAD (OMe)-FMK (zVAD) were obtained from MedChemExpress. Cell counting kit-8 (CCK-8) was purchased from Bimake. Annexin V-propidium iodide (PI) apoptosis kit was purchased from Beijing 4A Biotech Co., Ltd. Lactate dehydrogenase (LDH) assay kit was obtained from Nanjing Jiancheng Bioengineering Institute.

Cell lines and cell culture. Human neuroblastoma SH-SY5Y cell line and human non-small cell lung cancer A549 cell line were purchased from The Cell Bank of Type Culture Collection of the Chinese Academy of Sciences. The SH-SY5Y cell line was authenticated at 100% with an ATCC profile by Meide Huasheng Detection Technology Co (584164.b2bname.com/), using the short tandem repeat DNA profile method. SH-SY5Y cells were cultured in DMEM/F12 medium (HyClone; GE Healthcare Life Sciences), and A549 cells were maintained with F12 medium (HyClone; GE Healthcare Life Sciences). The two cell lines were supplemented with 10% fetal bovine serum (PAN-Biotech GmbH). The cells were incubated at 37˚C in a humidified atmosphere with 5% CO_2.

CCK-8 assay. CCK-8 assay was determined according to the manufacturer's protocol. Cells were seeded into a 96-well plate at a density of 3,000 cells/well, incubated for 24 h at 37˚C, and then exposed to dasatinib or DOX for 72 h at 37˚C. After co-incubation with CCK-8 for 2 h at 37˚C, the optical density (OD) values were read by a microplate reader (Bio-Ra Laboratories, Inc.) at 450 nm. Viability of the control group without drug was considered as 100%. Cell survival rates was calculated as follows: (%)=(OD of the drug-treated groups-OD of background)/(OD of the control group-OD of background) x100%. These rates were then plotted in GraphPad Prism 5 (GraphPad Software, Inc.).

Western blot analysis. Cells were lysed with lysis buffer, which contained 50 mM Tris-HCl (pH 7.5), 150 mM NaCl, 5 mM EDTA, 50 mM sodium fluoride, 1 mM dithiothreitol, 1% Triton X-100, 1 mM sodium orthovanadate and protease inhibitors. The protein concentration was measured using Quick Start™ Bradford 1x Dye Reagent (cat. no. 500-0205; Bio-Rad Laboratories, Inc.) with a microplate reader at 590 nm. A total of 20 μg protein/lane was separated via SDS-PAGE on a 10 or 12.5% gel. The proteins were transferred to a PVDF membrane (EMD Millipore), and then blocked with 5% skimmed milk at 4˚C for 1 h. The membrane was incubated with primary antibodies overnight at 4˚C, and incubated with the appropriate horseradish peroxidase-conjugated secondary antibody for 1 h at room temperature. The immunoreactive bands were visualized using the ECL Plus Western Blotting Detection System (Bio-Rad Laboratories, Inc.), and detected by an Amersham Imager 600 (GE Healthcare). The GSDME (1:2,000; cat. no. ab215191) and GSDMD (1:1,000; cat. no. ab210070) antibodies were obtained from Abcam. The antibodies against poly (ADP-ribose) polymerase 1 (PARP-1; 1:1,000; cat. no. 9532) and cleaved caspase-3

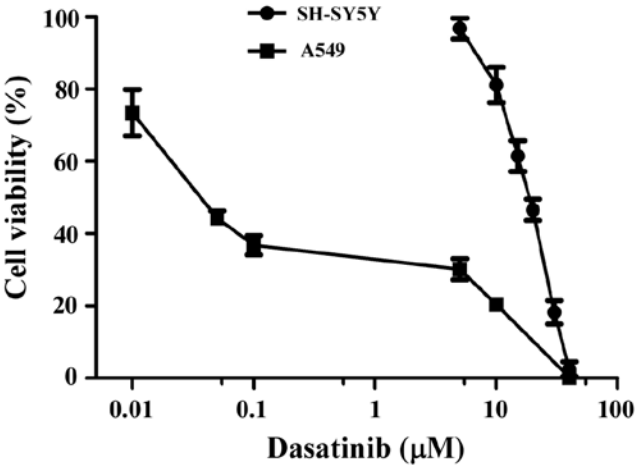

Figure 1. Rates of cell viability in SH-SY5Y and A549 cells. Cells were incubated with dasatinib for 72 h. Cell viability was determined by a CCK-8 assay. Results are expressed as the mean ± SD from three separate experiments.

(1:500; cat. no. 9664) were purchased from Cell Signaling Technology, Inc. The p53 (1:2,000; cat. no. sc-126) and β-actin (1:50,000; cat. no. sc-47778) antibodies were purchased from Santa Cruz Biotechnology, Inc. The secondary antibodies goat anti-rabbit IgG conjugated with HRP Conjugate (1:1,000, cat. no. HS101-01) and goat anti-mouse IgG conjugated with HRP (1:1,000, cat. no. HS201-01) were purchased from Beijing Transgen Biotech Co., Ltd.

Determination of apoptotic cells via Annexin V/PI staining. Cells were collected after exposure to the drugs for 24 h (SY5Y cells) and 48 h (A549 cells) and then stained with 5 μl Annexin V and final concentration of 2 μg/ml PI for 10 min at room temperature in the dark according to the manufacturer's protocols. The fluorescent intensities of the various groups were detected by a BD FACSCalibur flow cytometer (BD Biosciences) and were analyzed by CellQuest Pro software version 5.1 (BD Biosciences).

Identification of dead cells stained with PI. The PI-stained assay was used for the identification of dead cells. The cells were stained with 2 μg/ml PI in the dark for 10 min at room temperature after collection. The proportion of PI-positive cells was detected by a BD FACSCalibur flow cytometer and analyzed by CellQuest Pro software version 5.1.

LDH release assay. The LDH release assay was performed following the manufacturer's protocols. The total LDH present in the culture medium from the control group was set as 100%, and LDH release was calculated as follows: LDH release (%)=(OD of the drug-treated group-OD of blank control group)/(OD of the maximum group-OD of blank control group) x100%.

RNA interference. Small interfering (si)RNA against p53 was synthesized by Invitrogen; Thermo Fisher Scientific, Inc. The sequences of p53 were as follows: p53 siRNA: Forward, 5'-CAGCACATGACGGAGGTTGT-3' and reverse, 3'-TCA TCCAAATACTCCACACGC-5'; p53 siRNA: Forward, 5'-GAGGTTGGCTCTGACTGTACC-3' and reverse, 3'-TCC

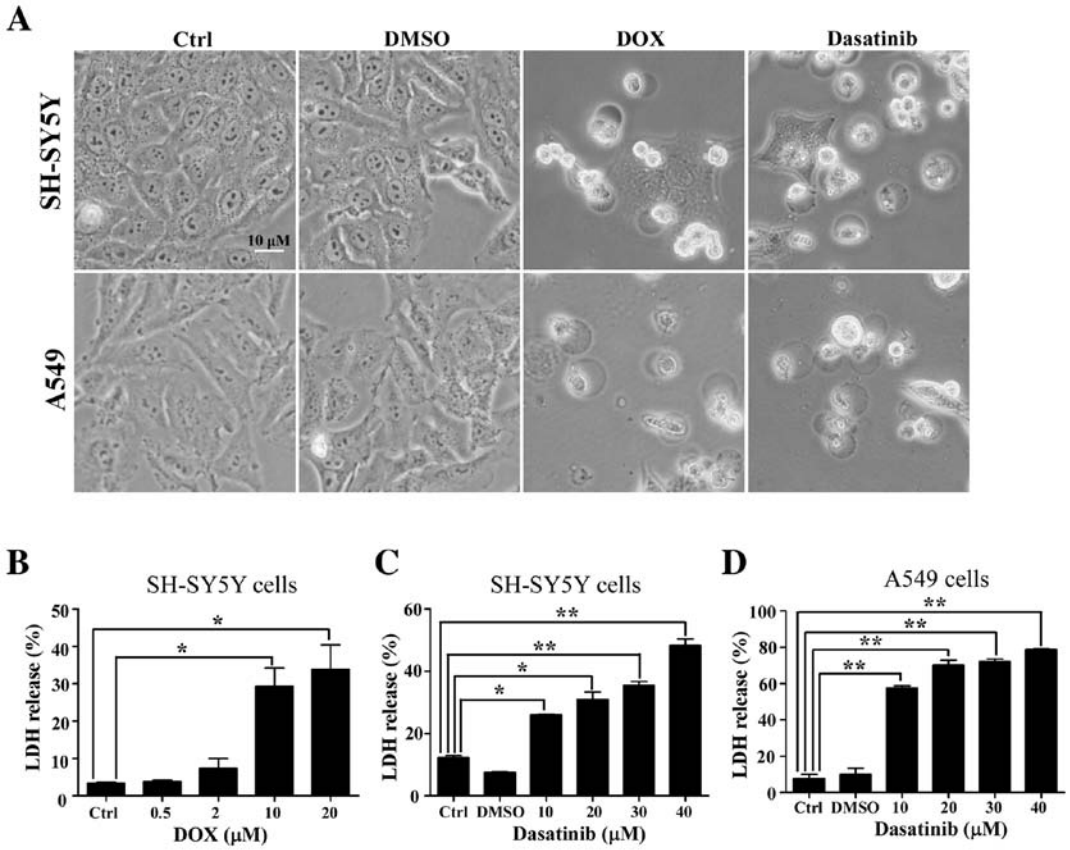

Figure 2. Induction of pyroptosis with dasatinib in SH-SY5Y and A549 cells. (A) Morphological changes in the DOX or dasatinib-induced pyroptosis. One representative result from three independent experiments is shown. (B) Levels of LDH release in the culture supernatant after exposure to DOX. Levels of LDH after exposure to dasatinib in (C) SH-SY5Y cells and (D) A549 cells. *P<0.05, **P<0.01 represents the drug treated groups vs. control group. DOX, doxorubicin; Ctrl, control; LDH, lactate dehydrogenase.

GTCCCAGTAGATTACCAC-5'. siRNA (100 pmol) was transfected into A549 cells using Lipofectamine® 2000 (Invitrogen; Thermo Fisher Scientific, Inc.) following the manufacturer's protocols. After 6 h transfection the cell were then maintained with refreshed culture medium for 18 h (the total transfection time was 24 h), the cells were then used for subsequent experiments. The p53 protein level was detected by western blot analysis.

Cell recovery assay. A549 cells were seeded into a 96-well plate at a density of 3,000 cells/well, incubated for 24 h at 37˚C. After 24 h of exposure to dasatinib at 37˚C, the drug was washed out. The cells were washed with phosphate buffer saline solution three times and then refreshed with new F12 culture medium. After incubation for 48 h at 37˚C, floating cells were transferred to a centrifugation tube, and the adherent cells were digested for 2 min with 0.1% trypsinase solution. Cells were then centrifuged for 5 min at 800 x g at room temperature, and then suspended in phosphate buffer. The cells were counted using a Coulter counter (Beckman Coulter, Inc.). The percentage of adherent cells was calculated as follows: %=Adherent cell number/(adherent cell number + floating cell number) x100%.

Statistical analysis. Data are presented as the mean ± SD from three independent experiments. Statistical analysis was calculated using ANOVA followed by Tukey's test using SSPS 19.0 (IBM Corp.). P<0.05 was considered to indicate a statistically significant difference.

Results

Dasatinib has distinct effects on the survival rates of SH-SY5Y and A549 cells. The effects of dasatinib treatment on cell survival rates were detected using the CCK-8 method. As shown in Fig. 1, SH-SY5Y cells were less sensitive to dasatinib than the A549 cells, and the IC_{50} value was 17.9 μM. Moreover, the range of viable concentrations of dasatinib was narrow in SH-SY5Y cells. Although the cell viability of SH-SY5Y cells was 81.1% with 10 μM dasatinib treatment, almost all of the cells died after exposure to 40 μM of the drug. In contrast to SH-SY5Y cells, A549 cells were more sensitive to dasatinib. The inhibition rate was 63.2% when the cells were treated with 0.01 μM dasatinib. However, the survival rates declined very slowly from 0.5 to 5 μM dasatinib treatment (Fig. 1).

Dasatinib treatment induces typical pyroptosis in SH-SY5Y and A549 cells. The typical characteristics of pyroptosis, including the large bubbled morphology, the generation of GSDME-N terminal fragments and the release of LDH (13), were significantly induced in the SH-SY5Y and A549 cells by DOX, a positive control drug for tumor chemotherapy (Figs. 2A and B and 3A). This is consistent with results from a previous study (13).

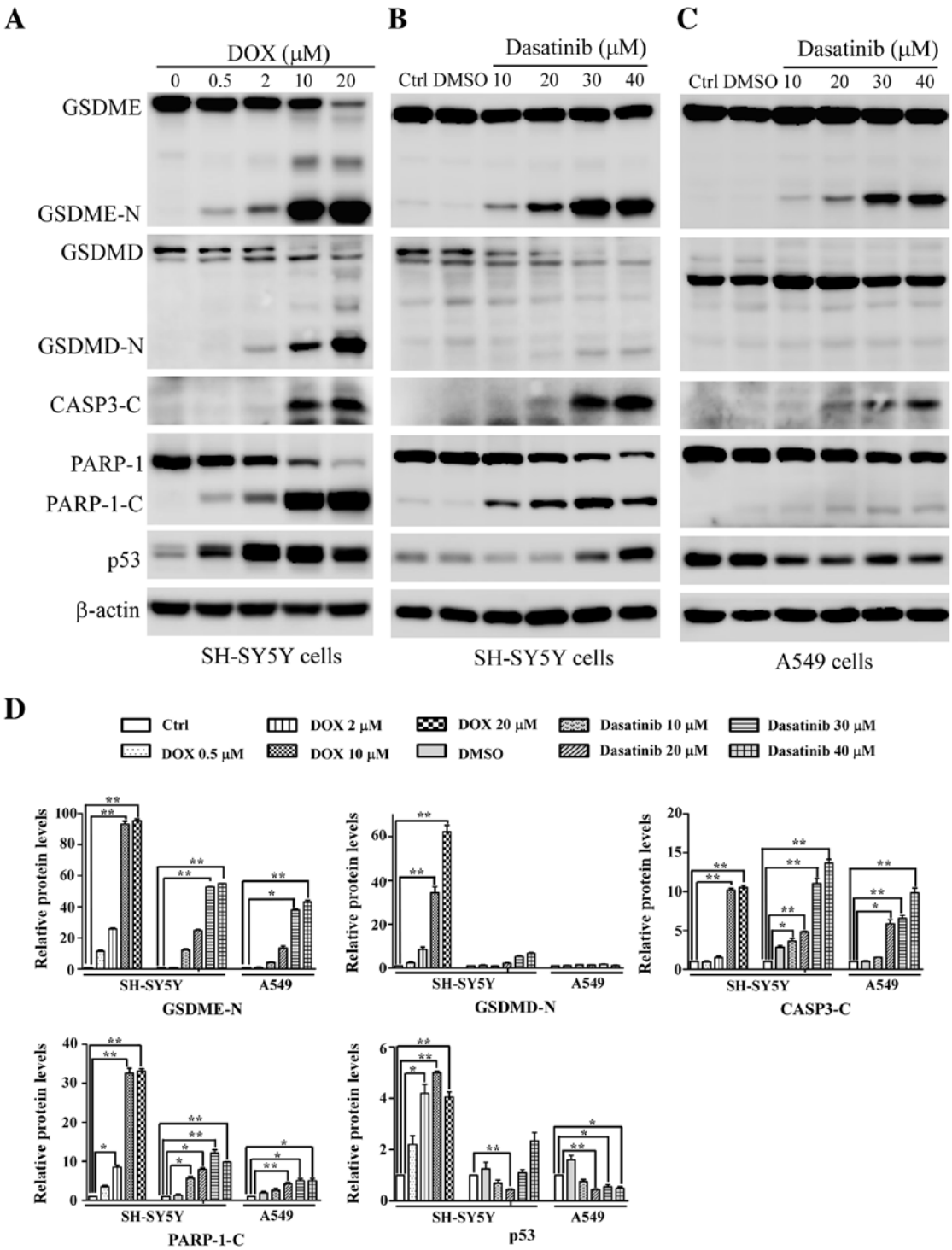

Figure 3. Changes in pyroptosis-related proteins detected with western blotting. SH-SY5Y cells were treated with (A) DOX or (B) dasatinib for 24 h, and (C) A549 cells were exposed to dasatinib for 48 h. One representative result from three independent experiments is shown. (D) Relative amounts of protein levels were quantified. *P<0.05, **P<0.01 represents the drug treated groups vs. control group. DOX, doxorubicin; Ctrl, control; GSDME, gasdermin E; GSDME-N N-terminal fragment of gasdemin E; GSDMD, gasdermin D; GSDMD-N, N-terminal fragment of gasdemin D; CASP3-C, cleaved caspase-3; PARP-1, poly (ADP-ribose) polymerase 1; PARP-1-C, cleaved fragment of PARP-1.

Similar characteristics were observed in SH-SY5Y and A549 cells after exposure to 30 or 40 μM dasatinib for 48 h (Figs. 2 and 3B and C). Interestingly, cleavage of GSDMD was detected in SH-SY5Y cells after treatment with either dasatinib or DOX (Fig. 3A and B). While there was a high level of LDH release in A549 cells following treatment with 10 μM dasatinib, very few GSDME-N fragments were detected (Figs. 2C and 3C).

Effect of dasatinib on p53 expression differs between SH-SY5Y and A549 cells. During apoptotic progression, the protein level of tumor suppressor gene *p53* gradually increases. Therefore, the present study investigated whether p53 is associated with dasatinib-induced pyroptosis. Increased p53 protein levels were observed in SH-SY5Y cells after treatment with dasatinib or DOX, especially in the DOX-treated group (Fig. 3A and B). By

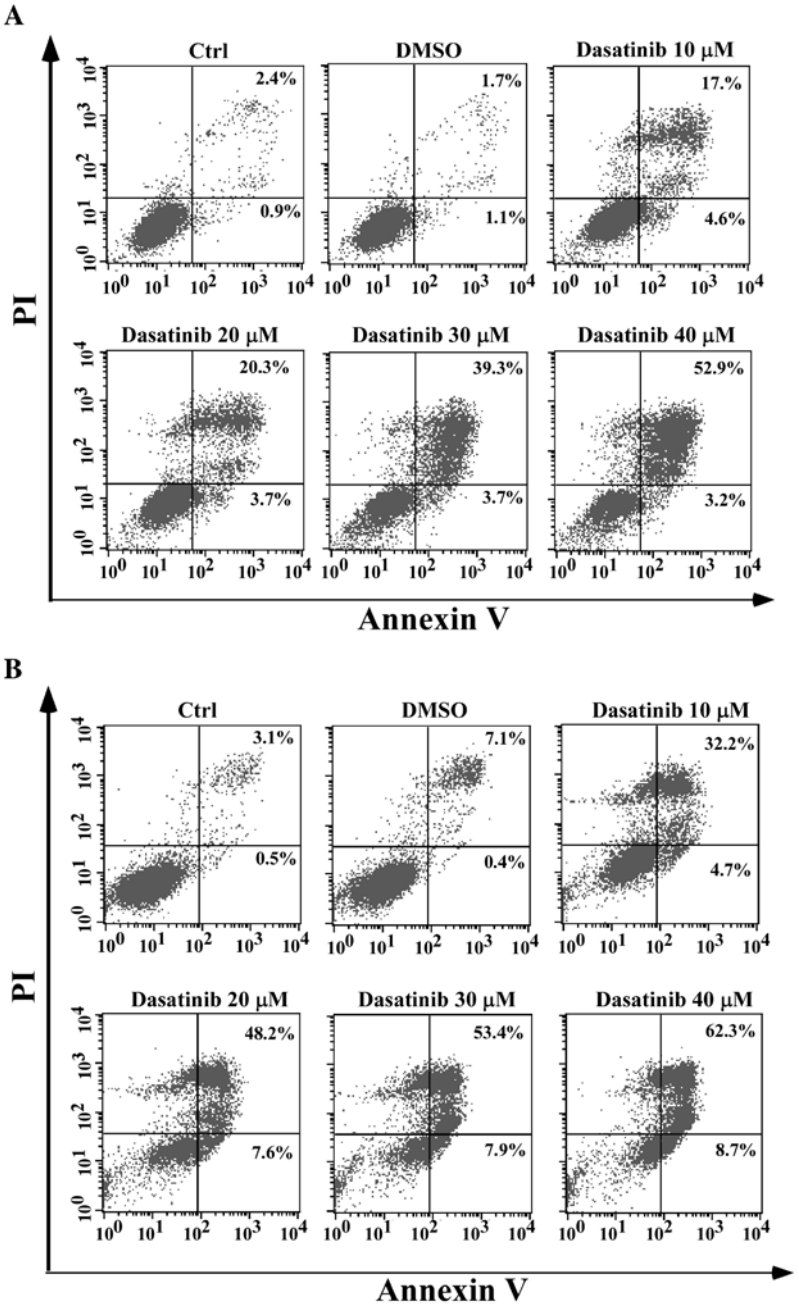

Figure 4. Cell apoptosis induced by dasatinib shown using Annexin V/PI staining. (A) SH-SY5Y cells after exposure to dasatinib for 24 h; (B) A549 cells after exposure for 48 h. One representative result from three independent experiments is shown. Ctrl, control; PI, propidium iodide.

contrast, A549 cells showed a reduction of p53 protein levels after exposure to dasatinib (Fig. 3C), suggesting differences in p53 expression between different cell lines in response to dasatinib treatment.

Dasatinib has distinct effects on the apoptotic response in SH-SY5Y and A549 cells. As pyroptosis is secondary to apoptosis and the cleavage of GSDME requires the activation of caspase-3 (13,14), apoptotic characteristics in relation to pyroptosis were investigated. In SH-SY5Y cells, apoptotic cells with Annexin V/PI staining, activation of caspase-3 and PARP-1 cleavage were associated with the occurrence of pyroptotic features after exposure to dasatinib, in a concentration-dependent manner (Figs. 3B and 4A). However, a notable apoptotic response following dasatinib treatment was observed in the A549 cells. A high percentage of Annexin V-stained cells and weak cleavages of caspase-3 and PARP-1 were detected following treatment with 10 μM dasatinib (Figs. 3C and 4B), inconsistent with the appearance of pyroptotic features. This suggests that different pyroptotic events occurred in the two cell lines after exposure to dasatinib.

Activation of caspase is required for dasatinib-induced pyroptosis. It has been reported that chemotherapy drug-induced pyroptosis is mediated by caspase-3 (13,14). To elucidate the role of caspase-3 in dasatinib-induced pyroptosis, the specific caspase-3 inhibitor zDEVD was used to inhibit activated caspase-3 in the cells. As shown in Fig. 5A, the cleavage

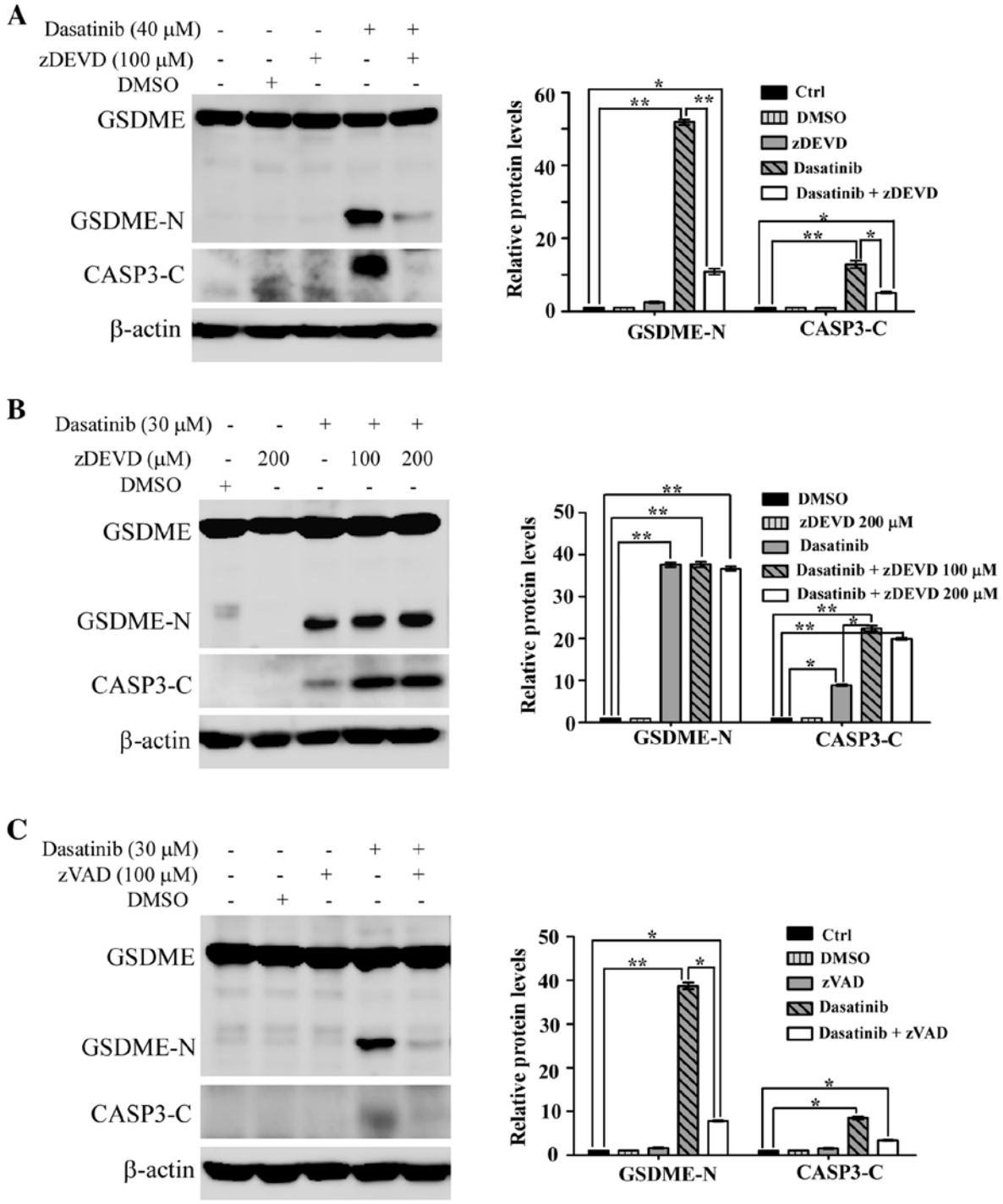

Figure 5. Requirement of caspase activation in dasatinib-induced pyroptosis. (A) Suppression of GSDME cleavage by pretreatment with caspase-3 inhibitor zDEVD when the SH-SY5Y cells were treated with 40 μm dasatinib. (B) Caspase-3 activity in A549 cells could not be inhibited by caspase-3 specific inhibitor zDEVD. (C) Inhibition of GSDME cleavage by pan-caspase inhibitor zVAD when the A549 cells were treated with 30 μm dasatinib. One representative result from three independent experiments is shown. *P<0.05, **P<0.01 represents the drug treated groups vs. control group. GSDME, gasdermin E; GSDME-N, N-terminal fragment of GSDME; zDEVD, caspase-3 inhibitor Z-DEVD-FMK; zVAD, pan-caspase inhibitor Z-VAD (OMe)-FMK; CASP3-C, cleaved caspase-3.

of both caspase-3 and GSDME was notably inhibited in SH-SY5Y cells pre-treated with zDEVD. This suggests that the activation of caspase-3 was essential to dasatinib-induced pyroptosis in SH-SY5Y cells.

Unexpectedly, the activation of caspase-3 and the generation of GSDME-N fragments were not suppressed by pre-treatment with zDEVD in A549 cells (Fig. 5B). However, the activation of caspase-3 and the generation of GSDME-N fragments in A549 cells were significantly suppressed by the pan-caspase inhibitor, zVAD (Fig. 5C).

Number of cells affects A549 cell sensitivity to dasatinib. As previously reported, the IC_{50} value of dasatinib in A549 cells was >5 μM, as measured by the MTT method (9). In

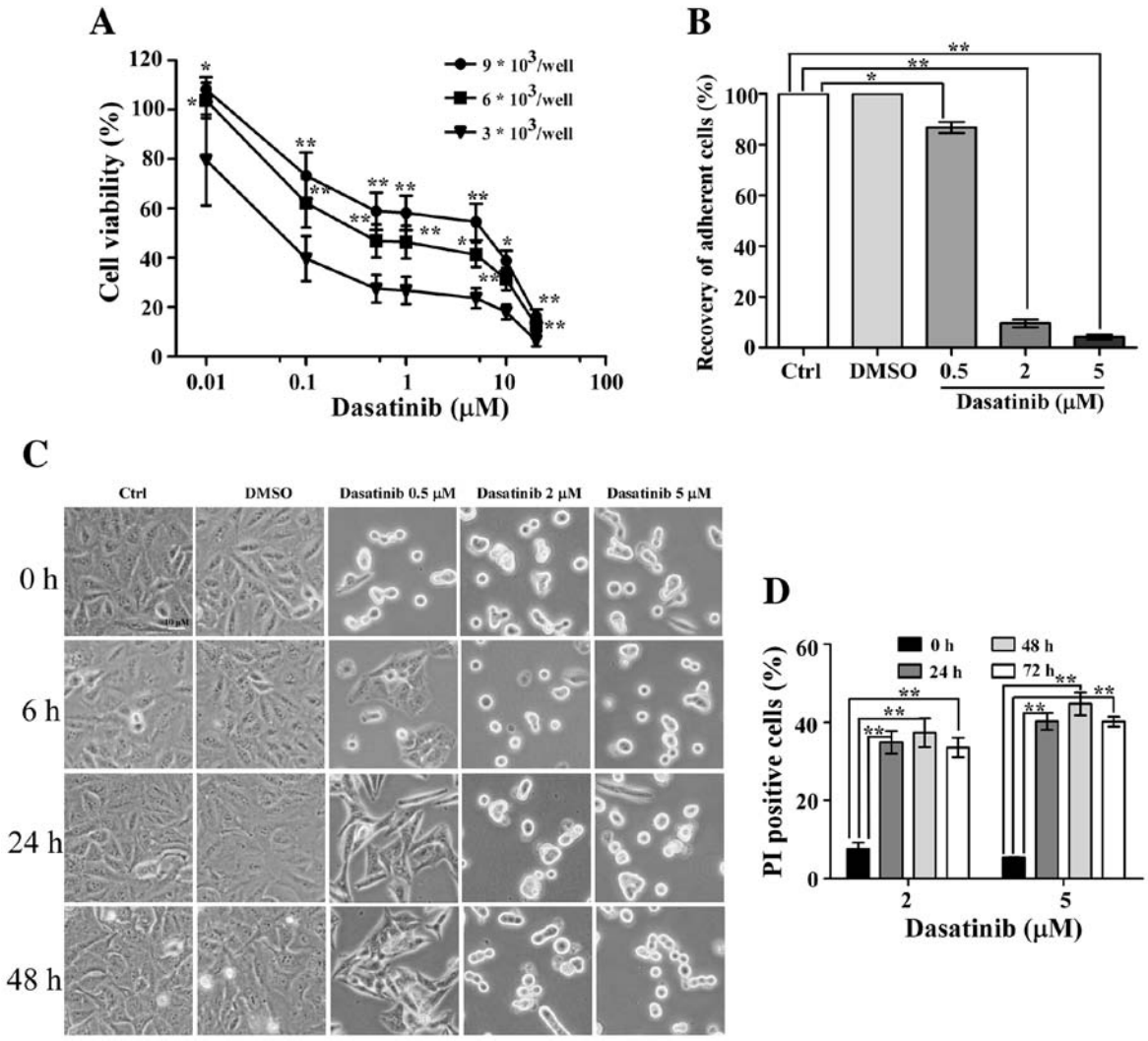

Figure 6. Effect of cell numbers on A549 cells sensitivity to dasatinib. (A) Cell viability rates comparing the seeding of different numbers of cells. Results are expressed as the mean ± SD from three separate experiments. (B) Recovery of cell morphology after exposure to dasatinib for 24 h (set as 0 h), or replacement with fresh medium for 6, 24 and 48 h. (C) Recovery rate of the adherent cells after medium refreshment for 48 h. (D) Proportion of PI positive cells when A549 cells were treated with 2 or 5 μM dasatinib for 24, 48 and 72 h. One representative result from three independent experiments is shown. *P<0.05, **P<0.01 represents the drug treated groups vs. control group. Ctrl, control; PI, propidium iodide.

the present study, the IC_{50} value was 0.04 μM, as determined by the CCK-8 method. Therefore, the reason for this notable difference was explored. A549 cells were seeded at various densities in a 96-well plate. The IC_{50} value of dasatinib in A549 cells was 2.5 μM at a seeding density of $9x10^3$ cells/well (Fig. 6A), suggesting that the number of cells affects cell viability following dasatinib treatment.

After 24 h of exposure to dasatinib, the drug was washed out and the cells were refreshed with a new culture medium. After 6 h of refreshment, some of the cells had recovered and adhered following 0.5 μM dasatinib treatment. The percentage of non-adherent cells was only 13.2% 48 h after the medium was replaced, suggesting that most of the A549 cells were still alive (Fig. 6B and C). However, <10% of the cells had adhered in the 2 or 5 μM dasatinib treatment groups 48 h after the medium was replaced. In order to differentiate the live cells from the dead cells, a PI single staining experiment was performed. These data showed high percentages of PI-stained cells after exposure to 2 or 5 μM dasatinib for 24 h. Furthermore, the proportion of PI positive cells remained stable after continuous incubation with dasatinib for 72 h (Fig. 6D).

Low concentration of dasatinib results in an increase of GSDME and GSDMD protein levels in A549 cells. During dasatinib-induced pyroptosis in A549 cells, it was found that the protein levels of GSDME and GSDMD increased slightly following treatment with 10 or 20 μM dasatinib (Fig. 3C). This led to further experiments to clarify whether dasatinib treatment itself results in the increase in protein levels. As shown in Fig. 7A, the protein levels of GSDME and GSDMD are significantly elevated in A549 cells following treatment with lower concentrations of dasatinib, and this increase was both concentration-dependent and -independent of changes in p53 protein levels. A time point experiment showed that the protein levels of GSDME and GSDMD increased after A549 cells following exposure to 0.2 μM dasatinib for 6, 12 or 24 h (Fig. 7B). However, the p53 protein levels in the dasatinib-treated groups were lower than those in the untreated groups.

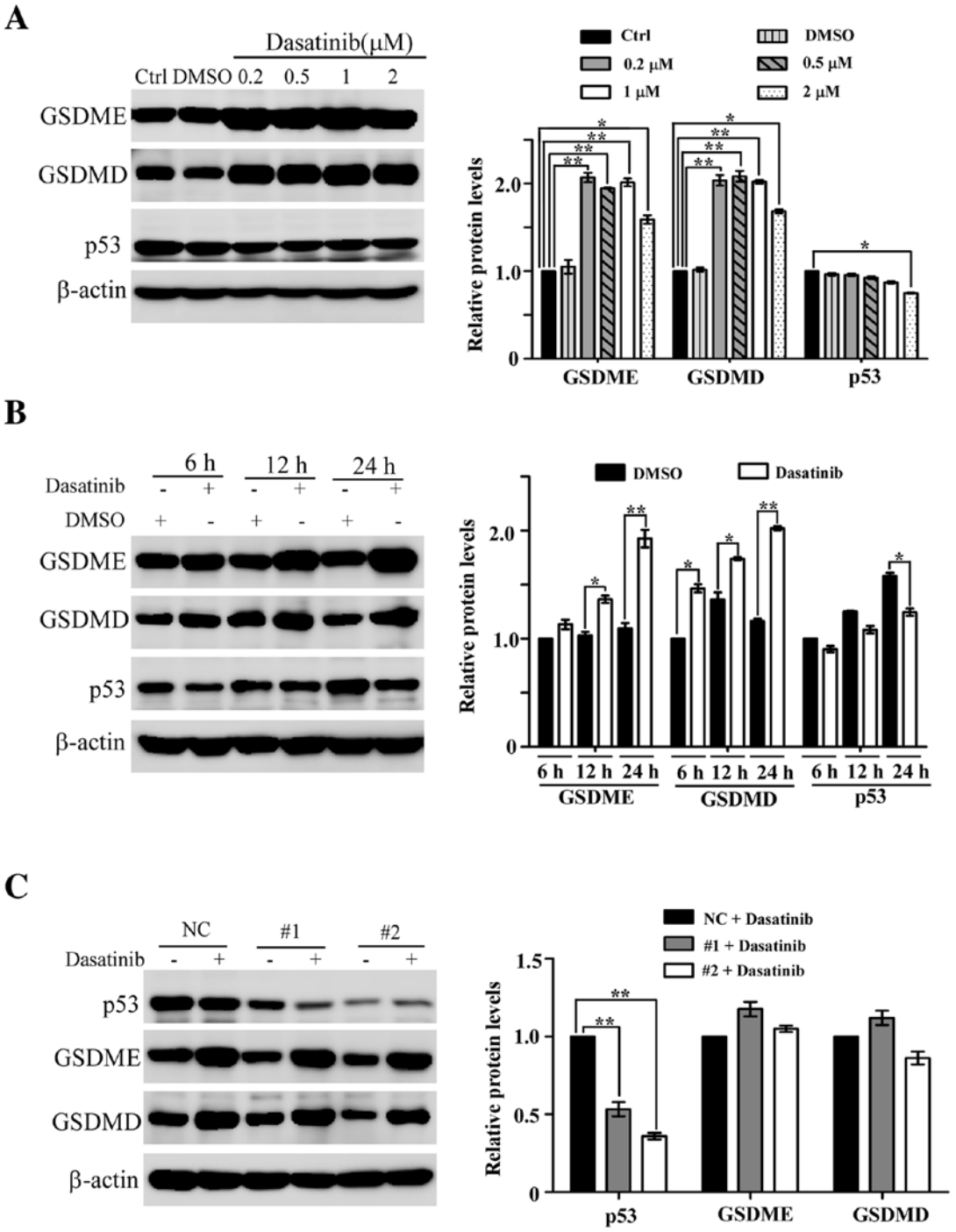

Figure 7. Increase in GSDME and GSDMD protein levels induced by low concentrations of dasatinib in A549 cells. (A) Increase in GSDME and GSDMD protein levels after treatment with low concentrations of dasatinib. (B) Time point expressions of GSDME and GSDMD protein after exposure to 0.2 μM dasatinib. (C) Decrease in p53 expression with RNA interference did not affect the expression of GSDME and GSDMD proteins after exposure to 0.5 μM dasatinib. The quantified results are expressed as the mean ± SD from three separate experiments. *P<0.05, **P<0.01 represents the drug treated groups vs. control group. NC, negative control; GSDME, gasdermin E; GSDMD, gasdermin D; Ctrl, control; siRNA, small interfering RNA.

To rule out the possibility that p53 participates in the regulation of dasatinib-related GSDME and GSDMD expression, RNA interference was used to knock down p53 in A549 cells. As shown in Fig. 7C, p53 protein levels were significantly reduced following siRNA transfection. The protein levels of GSDME and GSDMD were still upregulated in the p53 knockdown cells treated with 0.5 μM dasatinib for 24 h, demonstrating that the expression levels of GSDME and GSDMD are upregulated in response to dasatinib in a p53-independent manner.

Discussion

In the present study, the characteristics of dasatinib-induced pyroptosis in gasdermin-expressing human SH-SY5Y and A549 tumor cells, have been described. To the best of our knowledge, this is the first report showing that dasatinib can induce pyroptosis in tumor cells. Distinct pyroptotic features are also shown in dasatinib-treated A549 and SH-SY5Y cells. In addition to apoptosis, necroptosis and autophagy,

pyroptosis is another type of cell death induced by dasatinib action in both normal and tumor cells. As dasatinib is used in the treatment of leukemia, it is useful for the demonstration of dasatinib-induced pyroptosis in leukemia cell lines. However, to the best of our knowledge, there are few GSDME-expressing leukemia cell lines, including HL-60 cell and K562 cell lines (13). The significance of dasatinib-induced pyroptosis may be associated with micro-environment conditions in tumor cells, such as inflammation and therapy efficacy. It may be valuable to explain the mechanism of dasatinib in overcoming drug resistance in lung tumors, such as T790M resistance (18).

According to experiments in the present study, the positive control drug DOX always induced typical pyroptosis in several cell lines (data not shown), in contrast to dasatinib treatment. There are no differences in the induction of pyroptosis in both cell lines (Figs. 2 and 3). Apoptotic cells with Annexin V/PI staining were not accurately detected in the DOX-treated groups due to the overlapping of DOX auto-fluorescence and PI fluorescence.

As previously reported, GSDME meditates the induction of pyroptosis by chemotherapy agents (13,14). Another protein linked to pyroptosis, GSDMD, may play a role in tumor pathology. Treatment with dasatinib promoted the cleavage of both GSDME and GSDMD in SH-SY5Y cells (Fig. 3B). In non-small cell lung cancer, reduction of GSDMD can inhibit proliferation and is associated with an improved prognosis (19). Metformin can induce pyroptosis via the cleavage of GSDMD in human esophageal carcinoma cells (20). It is likely that more members of the gasdermin protein family will be shown to have roles in tumor pathology and therapy efficacy.

The question remains as to the reason for different GSDME-expressing tumor cells having distinct pyroptotic responses upon treatment with chemotherapy agents. In the present study, it was found that the caspase-3 specific inhibitor zDEVD did not suppress the activation of caspase-3 and the apoptotic rate is inconsistent with the cleavage of GSDME in A549 cells (Figs. 3C and 4B), therefore it is likely that other caspases are involved. Caspase-1 can induce apoptosis in GSDMD-deficient cells (21). Caspase-8 is a switch molecule for apoptosis, pyroptosis and necroptosis (22). It is commonly known that the continuous expression of p53 leads to the initiation of apoptosis after treatment with cytotoxic antitumor agents (23). As pyroptosis is secondary to apoptosis, high expression of p53 protein is proportional to the amount of cleavage fragments of GSDME in SH-SY5Y cells treated with dasatinib or DOX (Fig. 3). However, pyroptotic characteristics were also observed upon weak activation of caspase-3 and lower levels of p53 protein after exposure to dasatinib in A549 cells (Figs. 3C and 4B). The underlying mechanisms of these effects are currently being studied in our lab.

In the present study it is reported that low concentrations of dasatinib can result in an increase in protein levels of GSDME and GSDMD in A549 cells in a p53-independent manner (Fig. 7). To the best of our knowledge, this is the first study to show that dasatinib can induce to the upregulation of GSDME and GSDMD. Induction of GSDME expression by p53 was previously elucidated as a response to chemotherapy treatment, such as DOX or etoposide (15). The expression of GSDME is also elevated by glucocorticoids and forskolin, an activator of protein kinase A, however increased expression was not sufficient to induce apoptosis (24). Transfection of GSDME gene-carrying plasmids have been shown to increase apoptosis in heptocellular carcinoma cells (25), suggesting that GSDME has cytotoxic effects in tumor cells. It is unclear whether increased levels of GSDME can inhibit cell proliferation in the present study. Therefore, further investigation into the mechanism by which dasatinib modulates the expression of GSDME and GSDMD proteins is needed.

In the present study, it was discovered that higher concentrations of dasatinib is required for induction of pyroptosis in A549 cells compared with SH-SY5Y cells. A high percentage of apoptotic cells was detected after exposure to 10 μM dasatinib (Fig. 4), whereas it failed to induce cleavage fragment of GSDME in A549 cells (Fig. 3C). It may be that dasatinib can induce specific type of cell death in A594 cells. The cellular context of A549 cells may be responsible for it. High endogenous levels of nuclear factor erythroid 2-related factor 2 have been reported in A549 cells (26). In addition, high p53 expression was previously detected in A549 cells (27). As CCK-8 in this study for assessing cell survival, the sensitivity of A549 cells to dasatinib was influenced by cell numbers (Fig. 6). The possibility that culture volume affects the action of dasatinib on A549 cells has been ruled out (priliminary data not shown). Notably, suppression of Src activity in A549 cells in response to 150 nM dasatinib has been observed previously (9,28), suggesting that lower concentrations of dasatinib can play an inhibitory role. In a recent report, pyroptosis was shown to be induced in A549 cells by the chemotherapy agent cisplatin, but not by paclitaxel (29). These differences may be due to the heterogeneity of A549 cell populations as three sub-types were discovered according to cell morphological and molecular features (30).

In conclusion, dasatinib can induce typical pyroptosis in tumor cells and promote the expression of both GSDME and GSDMD in some types of tumor cells. These findings will broaden the understanding of the roles that pyroptosis plays in tumor cells. In addition, it is helpful to explain the various actions of dasatinib on normal and tumor cells.

Acknowledgements

Not applicable.

Funding

The study was supported by a grant from The Natural Scientific Foundation of China (grant no. 31471150).

Availability of data and materials

The datasets used during the present study are available from the corresponding author upon reasonable request.

Authors' contributions

QH conceived and designed the study. JZ and YC performed the experiments and analyzed the data. QH and JZ drafted the manuscript. All authors read and approved the final manuscript.

Ethics approval and consent to participate

All experimental protocols were approved by the Institute Review Board.

Patient consent for publication

Not applicable.

Competing interests

The authors declare that they have no competing interests.

References

1. Rossari F, Minutolo F and Orciuolo E: Past, present, and future of Bcr-Abl inhibitors: From chemical development to clinical efficacy. J Hematol Oncol 11: 84, 2018.
2. Shah NP, Tran C, Lee FY, Chen P, Norris D and Sawyers CL: Overriding imatinib resistance with a novel ABL kinase inhibitor. Science 305: 399-401, 2004.
3. Tu MM, Lee FYF, Jones RT, Kimball AK, Saravia E, Graziano RF, Coleman B, Menard K, Yan J, Michaud E, *et al*: Targeting DDR2 enhances tumor response to anti-PD-1 immunotherapy. Sci Adv 5: eaav2437, 2019.
4. Mestermann K, Giavridis T, Weber J, Rydzek J, Frenz S, Nerreter T, Mades A, Sadelain M, Einsele H and Hudecek M: The tyrosine kinase inhibitor dasatinib acts as a pharmacologic on/off switch for CAR T cells. Sci Transl Med 11: eaau5907, 2019.
5. Zhu Y, Tchkonia T, Pirtskhalava T, Gower AC, Ding H, Giorgadze N, Palmer AK, Ikeno Y, Hubbard GB, Lenburg M, *et al*: The Achilles' heel of senescent cells: From transcriptome to senolytic drugs. Aging Cell 14: 644-658, 2015.
6. Kirkland JL, Tchkonia T, Zhu Y, Niedernhofer LJ and Robbins PD: The clinical potential of senolytic drugs. J Am Geriatr Soc 65: 2297-2301, 2017.
7. Von Massenhausen A, Sanders C, Bragelmann J, Konantz M, Queisser A, Vogel W, Kristiansen G, Duensing S, Schrock A, Bootz F, *et al*: Targeting DDR2 in head and neck squamous cell carcinoma with dasatinib. Int J Cancer 139: 2359-2369, 2016.
8. Das J, Chen P, Norris D, Padmanabha R, Lin J, Moquin RV, Shen Z, Cook LS, Doweyko AM, Pitt S, *et al*: 2-aminothiazole as a novel kinase inhibitor template. Structure-activity relationship studies toward the discovery of N-(2-chloro-6-methylphenyl)-2-[[6-[4-(2-hydroxyethyl) -1-piperazinyl)]-2-methyl-4-pyrimidinyl]amino)]-1,3-thiazole-5-carboxamide (dasatinib, BMS-354825) as a potent pan-Src kinase inhibitor. J Med Chem 49: 6819-6832, 2006.
9. Johnson FM, Saigal B, Tran H and Donato NJ: Abrogation of signal transducer and activator of transcription 3 reactivation after Src kinase inhibition results in synergistic antitumor effects. Clin Cancer Res 13: 4233-4244, 2007.
10. Yang X, Wang J, Dai J, Shao J, Ma J, Chen C, Ma S, He Q, Luo P and Yang B: Autophagy protects against dasatinib-induced hepatotoxicity via p38 signaling. Oncotarget 6: 6203-6217, 2015.
11. Xu Z, Jin Y, Yan H, Gao Z, Xu B, Yang B, He Q, Shi Q and Luo P: High-mobility group box 1 protein-mediated necroptosis contributes to dasatinib-induced cardiotoxicity. Toxicol Lett 296: 39-47, 2018.
12. Shi J, Gao W and Shao F: Pyroptosis: Gasdermin-mediated programmed necrotic cell death. Trends Biochem Sci 42: 245-254, 2017.
13. Wang Y, Gao W, Shi X, Ding J, Liu W, He H, Wang K and Shao F: Chemotherapy drugs induce pyroptosis through caspase-3 cleavage of a gasdermin. Nature 547: 99-103, 2017.
14. Rogers C, Fernandes-Alnemri T, Mayes L, Alnemri D, Cingolani G and Alnemri ES: Cleavage of DFNA5 by caspase-3 during apoptosis mediates progression to secondary necrotic/pyroptotic cell death. Nat Commun 8: 14128, 2017.
15. Masuda Y, Futamura M, Kamino H, Nakamura Y, Kitamura N, Ohnishi S, Miyamoto Y, Ichikawa H, Ohta T, Ohki M, *et al*: The potential role of DFNA5, a hearing impairment gene, in p53-mediated cellular response to DNA damage. J Hum Genet 51: 652-664, 2006.
16. Lu H, Zhang S, Wu J, Chen M, Cai MC, Fu Y, Li W, Wang J, Zhao X, Yu Z, *et al*: Molecular targeted therapies elicit concurrent apoptotic and GSDME-dependent pyroptotic tumor cell death. Clin Cancer Res 24: 6066-6077, 2018.
17. Wang Y, Yin B, Li D, Wang G, Han X and Sun X: GSDME mediates caspase-3-dependent pyroptosis in gastric cancer. Biochem Biophys Res Commun 495: 1418-1425, 2018.
18. Watanabe S, Yoshida T, Kawakami H, Takegawa N, Tanizaki J, Hayashi H, Takeda M, Yonesaka K, Tsurutani J and Nakagawa K: T790M-selective EGFR-TKI combined with dasatinib as an optimal strategy for overcoming EGFR-TKI resistance in T790M-positive non-small cell lung cancer. Mol Cancer Ther 16: 2563-2571, 2017.
19. Gao J, Qiu X, Xi G, Liu H, Zhang F, Lv T and Song Y: Downregulation of GSDMD attenuates tumor proliferation via the intrinsic mitochondrial apoptotic pathway and inhibition of EGFR/Akt signaling and predicts a good prognosis in non-small cell lung cancer. Oncol Rep 40: 1971-1984, 2018.
20. Wang L, Li K, Lin X, Yao Z, Wang S, Xiong X, Ning Z, Wang J, Xu X, Jiang Y, *et al*: Metformin induces human esophageal carcinoma cell pyroptosis by targeting the miR-497/PELP1 axis. Cancer Lett 450: 22-31, 2019.
21. Tsuchiya K, Nakajima S, Hosojima S, Thi Nguyen D, Hattori T, Manh Le T, Hori O, Mahib MR, Yamaguchi Y, Miura M, *et al*: Caspase-1 initiates apoptosis in the absence of gasdermin D. Nat Commun 10: 2091, 2019.
22. Fritsch M, Günther SD, Schwarzer R, Albert MC, Schorn F, Werthenbach JP, Schiffmann LM, Stair N, Stocks H, Seeger JM, *et al*: Caspase-8 is the molecular switch for apoptosis, necroptosis and pyroptosis. Nature 575: 683-687, 2019.
23. El-Deiry WS: The role of p53 in chemosensitivity and radiosensitivity. Oncogene 22: 7486-7495, 2003.
24. Webb MS, Miller AL and Thompson EB: In CEM cells the autosomal deafness gene dfna5 is regulated by glucocorticoids and forskolin. J Steroid Biochem Mol Biol 107: 15-21, 2007.
25. Wang CJ, Tang L, Shen DW, Wang C, Yuan QY, Gao W, Wang YK, Xu RH and Zhang H: The expression and regulation of DFNA5 in human hepatocellular carcinoma DFNA5 in hepatocellular carcinoma. Mol Biol Rep 40: 6525-6531, 2013.
26. Homma S, Ishii Y, Morishima Y, Yamadori T, Matsuno Y, Haraguchi N, Kikuchi N, Satoh H, Sakamoto T, Hizawa N, *et al*: Nrf2 enhances cell proliferation and resistance to anticancer drugs in human lung cancer. Clin Cancer Res 15: 3423-3432, 2009.
27. Zhang HX, Chen Y, Xu R and He QY: Nrf2 mediates the resistance of human A549 and HepG2 cancer cells to boningmycin, a new antitumor antibiotic, in vitro through regulation of glutathione levels. Acta Pharmacol Sin 39: 1661-1669, 2018.
28. Sen B, Peng S, Tang X, Erickson HS, Galindo H, Mazumdar T, Stewart DJ, Wistuba I and Johnson FM: Kinase-impaired BRAF mutations in lung cancer confer sensitivity to dasatinib. Sci Transl Med 4: 136ra70, 2012.
29. Zhang CC, Li CG, Wang YF, Xu LH, He XH, Zeng QZ, Zeng CY, Mai FY, Hu B and Ouyang DY: Chemotherapeutic paclitaxel and cisplatin differentially induce pyroptosis in A549 lung cancer cells via caspase-3/GSDME activation. Apoptosis 24: 312-325, 2019.
30. Tièche CC, Gao Y, Bührer ED, Hobi N, Berezowska SA, Wyler K, Froment L, Weis S, Peng RW, Bruggmann R, *et al*: Tumor initiation capacity and therapy resistance are differential features of EMT-related subpopulations in the NSCLC cell line A549. Neoplasia 21: 185-196, 2019.